Engineering 6 (2020) 141–147

Contents lists available at ScienceDirect

Engineering

journal homepage: www.elsevier.com/locate/eng

Research
Rare Earth Permanent Magnets—Review

$ThMn_{12}$-Type Alloys for Permanent Magnets

G.C. Hadjipanayis [a], A.M. Gabay [a,*], A.M. Schönhöbel [a,b], A. Martín-Cid [b], J.M. Barandiaran [b], D. Niarchos [c]

[a] Department of Physics and Astronomy, University of Delaware, Newark, DE 19716, USA
[b] BCMaterials, Leioa 48940, Spain
[c] NCSR Demokritos, Agia Paraskevi 15341, Greece

ARTICLE INFO

Article history:
Received 16 July 2018
Revised 10 October 2018
Accepted 7 December 2018
Available online 31 May 2019

Keywords:
Permanent magnets
Rare earths permanent magnets
$ThMn_{12}$ structure

ABSTRACT

Iron-rich compounds with the tetragonal $ThMn_{12}$-type structure have the potential to meet current demands for rare-earth-lean permanent magnets with high energy density and operating temperatures of 150–200 °C. However, while it is normal for magnet technology to lag behind the development of underlying magnetic material, this gap has always been unusually large for $ThMn_{12}$-type magnets. The gap has widened further in recent years, as excellent combinations of intrinsic magnetic properties have been obtained in compounds synthesized with a smaller amount of structure-stabilizing elements (e.g., $SmFe_{11}V$ or $Sm_{0.8}Zr_{0.2}Fe_{9.2}Co_{2.3}Ti_{0.5}$) or with no such elements (i.e., $SmFe_{9.6}Co_{2.4}$ thin films). The search for promising compounds continues—with increasing help coming from theoretical calculations. Unfortunately, progress in the development of magnets beyond polymer-bonded interstitially modified powders remains marginal. The introduction of lanthanum (La) was found to stabilize low-melting-temperature minority phases in $Sm(Fe,Ti)_{12}$ alloys, thus allowing for liquid-phase sintering for the first time. The high reactivity of La, however, has apparently undermined the development of coercivity (H_c). A controlled crystallization of the initially suppressed $ThMn_{12}$-type phase makes "bulk" magnetic hardening possible, not only in Sm–Fe–V alloys (in which it has been known since the 1990s), but also is in La-added $(Ce,Sm)(Fe,Ti)_{12}$ alloys. The properties of the bulk-hardened alloys, however, remain unsatisfactory. Mechanochemically synthesized $(Sm,Zr)(Fe,Si)_{12}$ and $(Sm,Zr)(Fe,Co,Ti)_{12}$ powders may become suitable for sintering into powerful fully dense magnets, although not before a higher degree of anisotropy in both alloys and a higher H_c in the latter alloy have been developed.

© 2020 THE AUTHORS. Published by Elsevier LTD on behalf of Chinese Academy of Engineering and Higher Education Press Limited Company. This is an open access article under the CC BY-NC-ND license (http://creativecommons.org/licenses/by-nc-nd/4.0/).

1. Introduction

Tetragonal ferromagnetic compounds of the $ThMn_{12}$ type—that is, RT_{12} compounds in which R stands for rare earth element and T is mostly iron (Fe)—were recognized as promising hard magnetic materials as early as the 1980s. At that time, however, another iron-based 4f–3d compound, $Nd_2Fe_{14}B$, was being rapidly developed into powerful permanent magnets. Its higher saturation magnetization, relative ease of developing a useful coercivity (H_c), and phase equilibria favoring liquid-phase sintering and hot plastic deformation ensured the primary role of Nd–Fe–B, which now dominates the market of high-power permanent magnets. Recently, the rapidly growing demand for magnets operating at 150–200 °C and the 2010–2011 rare-earth supply crisis instigated an investigation of "new materials" [1], including the not-so-new RT_{12}. Since the composition of these materials has the lowest rare-earth content among the 4f–3d compounds, magnets based on these compounds may be less reliant on critical raw materials. Unlike $Nd_2Fe_{14}B$, RFe_{12}-type compounds are characterized by a negative value of the crystal field parameter A_2^0; thus, they exhibit the strongest uniaxial magnetocrystalline anisotropy for the rare earths R with a positive Stevens coefficient ϑ_2, such as samarium (Sm). At present, Sm is believed to be less vulnerable to supply restrictions than any other rare-earth metal [2]. If binary RFe_{12} alloys were realized, they would have the highest Fe content among the 4f–3d compounds and would thus be expected to exhibit the largest values of magnetization and energy density. One feature distinguishing current approaches to the development of RT_{12} hard magnetic materials from past approaches is that the former are supported by density functional theory (DFT) calculations and, most recently, by molecular dynamics simulations regarding

* Corresponding author.
E-mail address: gabay@udel.edu (A.M. Gabay).

https://doi.org/10.1016/j.eng.2018.12.011
2095-8099/© 2020 THE AUTHORS. Published by Elsevier LTD on behalf of Chinese Academy of Engineering and Higher Education Press Limited Company.
This is an open access article under the CC BY-NC-ND license (http://creativecommons.org/licenses/by-nc-nd/4.0/).

the selection of stable structures with high magnetization. Many recent and ongoing experiments are pursuing RT_{12} compounds with a higher concentration of magnetic Fe and cobalt (Co) atoms. Yet another avenue of research is aimed at the incorporation of more abundant and underused rare earths cerium (Ce) and lanthanum (La), or non-critical zirconium (Zr), even though the non-magnetic atoms of these elements would not contribute to the magnetization and anisotropy of the compounds. The major challenge, however, lies in converting RFe_{12} compounds with promising fundamental magnetic properties into functional and preferably fully dense and anisotropic magnets, which could compete with the nearly perfected Nd–Fe–B. In this paper, we provide an overview of our ongoing research in the context of other recent developments in RT_{12} compounds and magnets.

2. Crystal structure, magnetism, and early efforts to develop H_c

Fig. 1 depicts the $ThMn_{12}$ unit cell; the cell incorporates two formula units. The two large thorium (Th) atoms occupy a single 2*a* site and the 24 small manganese (Mn) atoms are evenly distributed between the 8*i*, 8*j*, and 8*f* sites. The tetragonal RT_{12} structure—like the rhombohedral and hexagonal R_2T_{17} structures, the monoclinic R_3T_{29} structure, and the disordered hexagonal solid solution known for its $TbCu_7$ prototype—can be derived from the hexagonal RT_5 structure by replacing part of the R atoms with pairs of the T atoms. When T = Fe, a third element, M, is needed to stabilize the RT_{12} structure, as $R(Fe,M)_{12}$. The large transition metal atoms (M = Ti, V, Nb, Mo, Ta, W) occupy the 8*i* sites of $R(Fe,M)_{12}$; these sites are characterized by the largest Wigner–Seitz cell. The *sp* atoms (M = Al, Si) prefer the 8*f* sites, which allow for two direct bonds with the R atoms [3,4]. Up to one light element atom (i.e., H, N, or C) may occupy the interstitial position in the RT_{12} cell, but the resulting modified lattice is metastable; it can only exist as long as the formation of the more stable rare-earth hydrides, nitrides, or carbides is suppressed by kinetic factors. Interstitial modification with nitrogen, in particular, increases the Curie temperature and changes the sign of the A_2^0 crystal field parameter from negative to positive. Thus, unlike $R(Fe,M)_{12}$ compounds, $R(Fe,M)_{12}N_x$ nitrides exhibit a strong uniaxial anisotropy when R = praseodymium (Pr) or neodymium (Nd) ($\vartheta_2 < 0$) [3].

Early attempts to develop plausible hard magnetic properties in the 1:12 alloys produced an H_c of 11–12 kOe (1 Oe = 79.6 A·m^{-1}) in isotropic melt-spun or high-energy-milled $Sm(Fe,Ti,V)_{12}$ alloys [5,6] and a full-density-projected maximum energy product $(BH)_{max}$ of 21 MG·Oe (1 MG·Oe = 7.96 kJ·m^{-3}) in $Nd(Fe,Mo)_{12}N_x$ anisotropic powders [7]. Experiments with sintering powdered $Sm(Fe,M)_{12}$ alloys into fully dense magnets were not very successful, even when the sintering was performed in a Sm atmosphere [8].

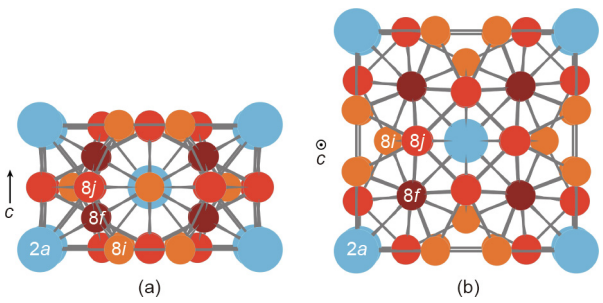

Fig. 1. Schematic representation of a $ThMn_{12}$ unit cell along (a) the [100] direction and (b) the [001] direction *c*.

3. RFe_{12} materials since 2010

3.1. Computational approaches

First-principle calculations based on DFT make it possible to search for promising $R(Fe,M)_{12}X$ compounds over a great variety of R, M, and X elements [9,10]. However, the first attempt at true high-throughput computational screening, in which the structures were generated and analyzed automatically [10], was undermined by inaccurate assumptions about the site occupancies of the M atoms (only the 8*i* sites) and the valence state of the Ce ions (Ce^{3+} instead of the mixed-valence state between Ce^{3+} and Ce^{4+}), and by incorrect evaluation of the stability of the compound based on the formation energy of only this compound. A specific target of these theoretical studies was the interstitial modification, particularly with X elements such as oxygen (O), fluorine (F) [11], and lithium (Li) [12], which would be difficult to study experimentally. A strong uniaxial anisotropy that is less temperature dependent than that of the $NdFe_{12}N$ nitride was predicted for the hypothetical $SmFe_{12}Li$ [12]. It is unlikely, however, that these interstitially modified compounds—even if synthesized—will be more stable than the $R(Fe,M)_{12}H$ hydrides and $R(Fe,M)_{12}N$ nitrides; thus, the range of their applications will be rather limited. An arguably more worthwhile aim is to identify the conditions for stable $R(Fe,M)_{12}$ compounds with minimal or no substitution for the magnetic Fe atoms. The formation of $R(Fe,M)_{12}$ structures with various M elements, the stabilities of RFe_{12} with various R elements including scandium (Sc), Zr, and hafnium (Hf), and the effect of hydrostatic pressure have been analyzed [13,14]. These calculations have confirmed what was already known from experiments: For any R, the hypothetical binary RFe_{12} structure is less stable than the R_2Fe_{17} structure. At the same time, the difference between the RFe_{12} and R_2Fe_{17} formation energies is reduced for R = Nd or Sm if these elements are partially replaced with Zr, yttrium (Y), dysprosium (Dy), holmium (Ho), erbium (Er), or thulium (Tm). Thus, although substitution for the R element does not make RT_{12} structures stable, it may decrease the minimum necessary substitution for the T element. In addition to DFT calculations, molecular dynamics, which uses the classical equations of motion to predict the dynamic evolution of atoms in a crystal structure, has recently become another approach to assess the stability of the $R(Fe,M)_{12}$ structure with a minimal percentage of M [15].

3.2. Epitaxially grown RFe_{12} and $R(Fe,Co)_{12}$ films with high magnetization

The presence of a binary $SmFe_{12}$ compound stabilized with an underlayer in an epitaxially grown thin film was first reported in 1991 [16]. As expected for an undiluted Fe component, it exhibited a high but not exceptional saturation magnetization. The full significance of excluding the third structure-stabilizing element became clear only in the last three years, after the preparation and characterization of $NdFe_{12}N_x$ and $Sm(Fe,Co)_{12}$ epitaxial films [17–19]. Table 1 compares the basic magnetic properties, Curie temperature (T_C), saturation magnetization ($4\pi M_s$), and magnetic anisotropy field (H_a) of these films with the properties of $Nd_2Fe_{14}B$ and $Nd_2(Fe,Co)_{14}B$. The comparison demonstrates that $ThMn_{12}$-type compounds exhibit potential for greater magnetic energy density. The theoretical limit of the $(BH)_{max}$ of $SmFe_{9.6}Co_{2.4}$ films can be estimated as $(2\pi M_s)^2$ = 79 MG·Oe, which is a record high value. At the practically important elevated temperatures of 150–200 °C, this superiority becomes even greater, due to the low T_C of $Nd_2Fe_{14}B$ and the highly detrimental effect of Co on the $H_a(T)$ dependence of $Nd_2(Fe,Co)_{14}B$ [20].

High-magnetization thin films exhibit an H_c of 4–5 kOe [18,29]. Infiltration of the films with copper (Cu) and gallium (Ga), aimed at

Table 1
Room-temperature magnetic properties and Curie temperatures reported for selected $Nd_2Fe_{14}B$-type and $ThMn_{12}$-type compounds.

Nominal composition[a]	Form[b]	T_C (°C)	$4\pi M_s$ (kG)	H_a (kOe)	References
$Nd_2Fe_{14}B$	Any	313	16.0	73	[20,21]
$Nd_2(Fe_{0.8}Co_{0.2})_{14}B$	Any	498	16.3	69	[20,22]
$NdFe_{12}N_x$	Film	~550	17.0	60–80	[17,18]
$SmFe_{9.6}Co_{2.4}$	Film	586	17.8	120	[19]
$Nd_{0.7}Zr_{0.3}(Fe_{0.75}Co_{0.25})_{11.5}Ti_{0.5}N_x$	Powder	> 570	16.7	66	[23,24]
$Sm_{0.92}Zr_{0.08}(Fe_{0.75}Co_{0.25})_{11.35}Ti_{0.65}$	Any	570	14.7	> 90	[25]
$Sm_{0.8}Y_{0.2}(Fe_{0.80}Co_{0.20})_{11.4}Ti_{0.6}$	Any	547	15.0	110	[26]
$Sm_{0.8}Zr_{0.2}(Fe_{0.80}Co_{0.20})_{11.5}Ti_{0.5}$	Any	557	15.3	84	[27]
$Sm_{0.8}Zr_{0.2}(Fe_{0.75}Co_{0.25})_{11.5}Ti_{0.5}$	Any	607	15.8	74	[28]

[a] Some of the reports indicate the presence of impurity phases, but do not account for their effect on the composition of the principal phase.
[b] Form in which the material can be synthesized; "any" indicates an absence of known restrictions.

the magnetic insulation of $Sm(Fe,Co)_{12}$ crystallites, reportedly increases the H_c to 8 kOe, even though no continuous grain-boundary phase has actually been formed [29]. These H_c values are still quite low compared with the values of more than 30 kOe that are developed in the Nd–Fe–B thin films [30]. The real problem, however, is not the relatively low H_c, but the current inability to prepare bulk $NdFe_{12}N_x$ and $Sm(Fe,Co)_{12}$ alloys without the stabilizing effect of an underlayer. As long as these compounds are only available as thin films, they cannot be used as permanent magnets: The shape of the thin films does not allow for the utilization of their stored magnetic energy.

3.3. $SmFe_{12-x}V_x$ compounds with increased magnetization

Early studies of $RFe_{12-x}M_x$ compounds established the minimum x values as approximately 0.5 for M = molybdenum (Mo) or tantalum (Ta), 0.7 for M = niobium (Nb) or tungsten (W), 1 for M = titanium (Ti), 1.5 for M = vanadium (V) or chromium (Cr), and 2 for M = silicon (Si). For reasons that are still not well understood, $Sm(Fe,V)_{12}$ alloys are most susceptible to the development of viable coercivities. In an attempt to obtain $SmFe_{12-x}V_x$ alloys with an x smaller than reported earlier [3,31,32], we have studied the phases and magnetic properties in alloys with x varying from 0.5 to 2. The alloys were prepared by arc-melting followed by homogenization at temperatures in the range of 900–1100 °C for 1–4 d. After the appropriate homogenization, a nearly pure $ThMn_{12}$-type structure was obtained for $x = 1$; the corresponding X-ray diffraction (XRD) spectrum is shown in Fig. 2(a). The strong [002] peak observed in the spectrum recorded for the oriented powder in Fig. 2(b) confirms that the magnetocrystalline anisotropy of the compound is uniaxial. The reduction of x in the $SmFe_{12-x}V_x$ compound from 2 to 1 increases the T_C from 321 to 361 °C, the saturation magnetization from 83 emu·g^{-1} (1 emu·g^{-11} = 1 A·m^2·kg^{-11}) (8.1 kG) to 115 emu·g^{-1} (11.2 kG), and the anisotropy field from 98 to 110 kOe.

3.4. Nitrogenization of $R(Fe,M)_{12}$ compounds with M = V, Mo, and Si

Despite the vast amount of data that has been gathered on Co-substituted $R(Fe_{1-x}Co_x,M)_{12}$ alloys and, on the other hand, on interstitially modified $R(Fe,M)_{12}N_y$ nitrides, the effect of Co substitution on the properties of these nitrides remained the subject of controversy for a long time. A recent study [33] demonstrated that small Co substitutions improve all the basic magnetic properties of the $NdFe_{10.5-x}Co_xMo_{1.5}N_y$ nitrides, whereas large Co substitutions are detrimental not only for the $4\pi M_s$ and H_a, but even for the T_C. The improvement was confirmed for the $NdFe_{10.5-x}Co_xV_{1.5}N_y$ nitrides, with the substitution $x = 0.9$ increasing the saturation magnetization by 11%, to 138.5 emu·g^{-1} [33].

Until recently, interstitial modification with nitrogen had only been reported in $R(Fe,M)_{12}$ compounds with M represented by the transition metals. Apparently, the gas–solid nitrogenization reaction does not occur at 1 atm (1 atm = 1.01 × 10^5 Pa) nitrogen pressure when M = Si, Al. However, after increasing the pressure to 20 atm, $CeFe_{10}Si_2N_y$ [34] and $Nd_{0.6}Zr_{0.4}Fe_{10}Si_2N_y$ nitrides were successfully synthesized. The latter nitride was found to have an H_a of 53 kOe compared with 29 kOe for the parent compound. Fig. 3 presents thermogravimetric scans demonstrating a two-phase formation of the interstitially modified structure that is characterized by a higher T_C.

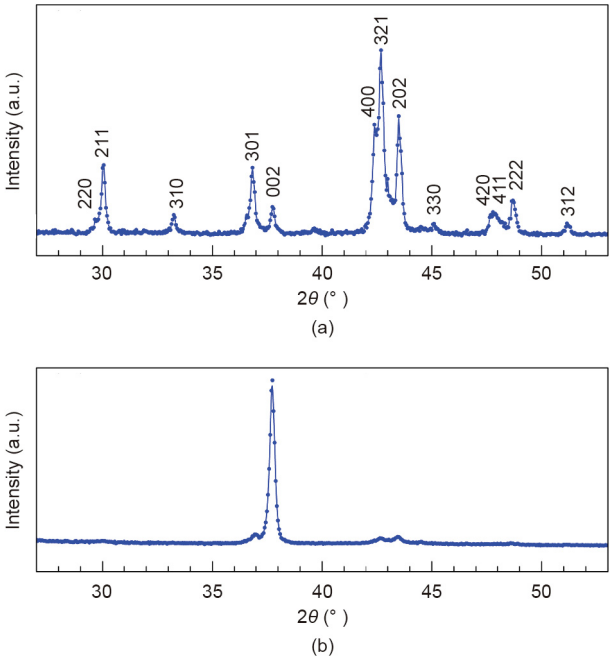

Fig. 2. XRD spectra of $SmFe_{11}V$ (a) randomly oriented and (b) field-oriented powders. θ: the X-rays incident angle.

3.5. $R_{1-v}A_v(Fe,Co,M)_{12}$ compounds with increased magnetization and reduced R content (A = Zr, Y)

Recent experimental findings have indicated that the $ThMn_{12}$-type structure $R(Fe,Co)_{12-x}Ti_x$, R = Nd or Sm can be obtained with $x < 1$ when part of R is replaced by Zr [23,24,28] or Y [26]. This effect was explained through the similarity between the local lattice changes for Zr atoms occupying the 2*a* sites and Ti atoms occupying the 8*i* sites [35]. DFT calculations [13] have also indicated that partial replacement of Nd or Sm with Zr and Y should decrease the difference between the higher formation energy of the RFe_{12} structure and the lower formation energy of the R_2Fe_{17} structure. Table 1 presents the properties reported for Zr- and

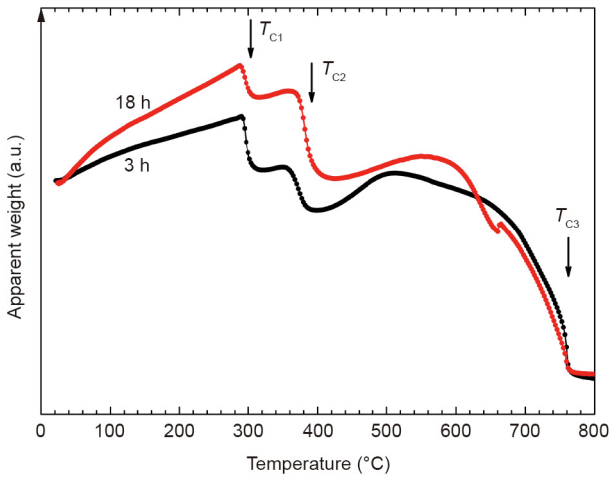

Fig. 3. Apparent weight of $Nd_{0.6}Zr_{0.4}Fe_{10}Si_2N_y$ alloys heated in a thermogravimetric analyzer in a constant magnetic field after nitrogenization at 550 °C for 3 h (black) and 18 h (red) under 20 atm nitrogen gas. T_{C1}, T_{C2}, and T_{C3} indicate the Curie temperatures of the parent phase, nitride phase, and body-centered cubic (bcc) Fe–Si impurity phase, respectively.

Y-substituted $R_{1-v}A_v(Fe,Co)_{12-x}Ti_x$ compounds with $x < 1$. The room-temperature saturation magnetization of these compounds approaches or even exceeds that of $Nd_2Fe_{14}B$; at 150–200 °C, both the $4\pi M_s$ and H_a of $ThMn_{12}$-type compounds are superior [27]. It should be noted that the alloys prepared with $x = 0.5$ contained impurity phases including the α-Fe phase; it was claimed that the $4\pi M_s$ values listed in Table 1 accounted for the impurities, but the actual compositions of the corresponding $ThMn_{12}$-type phases are likely to have $x > 0.5$. No experiments aimed at the development of an H_c in these "Ti-lean" compounds have been reported yet, and the presence of the soft magnetic α-Fe phase in alloys with $x = 0.5$ is unfavorable for such efforts. Our attempt to prepare magnetically hard "Ti-lean" alloy via mechanochemistry is described in Section 4.3.

In Zr-substituted $R_{1-v}Zr_vFe_{10-x}Si_x$ compounds, the x value cannot be decreased below 1.6, which is much higher than in the compounds stabilized by Ti. What is remarkable about the Si-stabilized $ThMn_{12}$-type structures is that they can sustain a complete replacement of the rare-earth element R with Zr [36]. The rare-earth-free $Zr(Fe,Si)_{12}$ compounds are, apparently, metastable and their anisotropy is believed to be too weak for permanent magnet materials. However, as an answer to the overreliance of permanent magnets on the "critical" rare-earth elements, very rare-earth-lean $R_{1-x}Zr_x(Fe,Si)_{12}$ compounds with R = Nd [37] and Sm [38] may be of interest.

4. Development of RFe_{12} magnets

4.1. Sintering

With the exception of "intrinsically hard" $R(Co,M)_5$ compounds, the development of H_c in uniaxially anisotropic ferromagnetic 4f–3d compounds is achieved through refinement of the crystallites. In the practice of permanent magnet manufacturing, this refinement typically involves rapid solidification or powder metallurgy. Although the former has been proven to work for $ThMn_{12}$-type alloys [5], only the latter—that is, milling followed by magnetic-field alignment and sintering—can reliably ensure textured and fully dense materials. Traditional sintering of $Nd(Fe,M)_{12}N_x$ nitrides is ruled out by the inherent instability of these compounds. Apart from the high vapor pressure of Sm [8], the most obvious obstacle to manufacturing sintered magnets with $Sm(Fe,M)_{12}$ alloy as the principal phase is the soft magnetic phases that surround that compound on the equilibrium phase diagram [3]. In contrast, sintering of Nd-Fe-B magnets is greatly facilitated by the eutectic reaction between the $Nd_2Fe_{14}B$ and Nd phases; the emerging liquid assists in the densification of the press–compacts and allows for a partial or even complete insulation of the $Nd_2Fe_{14}B$ grains with non-magnetic phases.

La is unique among the rare-earth elements in that it does not form binary compounds with Fe, and has been shown to avoid $ThMn_{12}$-type structures [38]. It is, therefore, conceivable that the addition of La to $R(Fe,M)_{12}$ alloys will lead to a eutectic mixture of the $R(Fe,M)_{12}$ and La phases, thus facilitating both the densification and development of H_c through sintering. To test this hypothesis, a $Sm_8La_5Fe_{80}Ti_7$ alloy, which may also be presented as $(Sm_{0.084}Fe_{0.842}Ti_{0.074})_{95}La_5$, was prepared via arc-melting and homogenized for 3 h at 1050 °C. At this stage, according to the XRD characterization shown in Fig. 4(a) (spectrum ①), the $ThMn_{12}$-type phase co-exists with what appears to be metallic La. The alloy was ball-milled under toluene for 1.5–10 h. The resulting fine powders were wet-pressed in a magnetic field, then sealed in argon-filled quartz capsules and sintered for 3 h at 1050 °C. The phases and properties of the sintered alloys appear to be strongly influenced by the oxidation of the highly reactive metallic La during the milling. As the milling time increased, an increasing amount of a rare-earth oxide (perhaps La oxide?) could

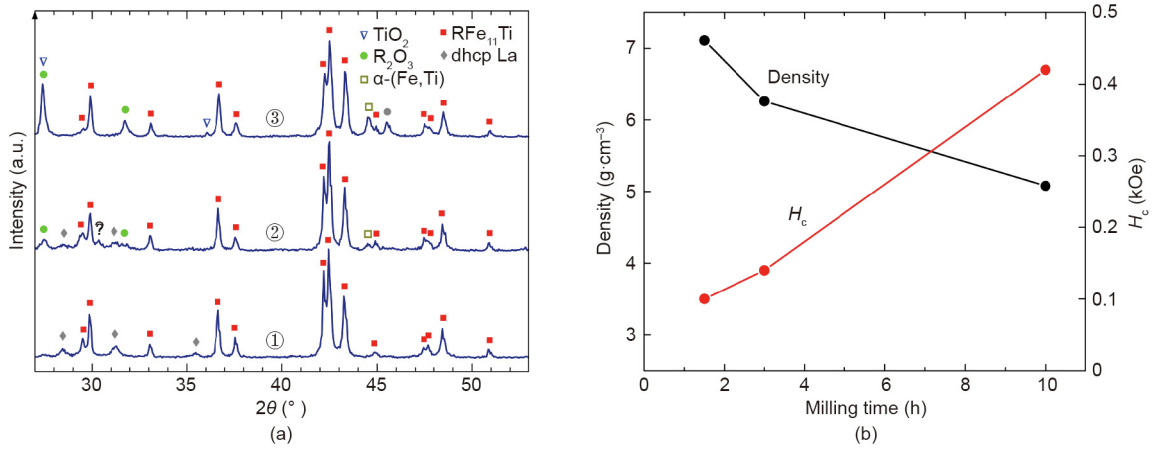

Fig. 4. Characterization of $(Sm_{0.084}Fe_{0.842}Ti_{0.074})_{95}La_5$ alloy subjected to homogenization, ball-milling, and sintering. (a) XRD spectra of ① homogenized alloy, ② alloy sintered after milling for 1.5 h, and ③ alloy sintered after milling for 10 h; (b) properties of the sintered alloys as a function of milling time. Double hexagonal close packed (dhcp) structure of metallic La was identified tentatively.

be detected in the sintered alloys, while the XRD reflections corresponding to the double hexagonal close packed (dhcp) La decreased and eventually disappeared (Fig. 4(a)). It is believed that the eutectic reaction between the $R(Fe,Ti)_{12}$ and La phases facilitated densification of the powders milled for 1.5–3 h; the corresponding density values are presented in Fig. 4(b). The electron micrographs shown in Fig. 5 reveal that the 3–20 μm as-milled particles with sharp edges evolve into 5–30 μm grains of the $R(Fe,Ti)_{12}$ phase with well-developed facets. The minority R-rich phases are characterized by very large La/R ratios—0.92 for the oxide phase and 0.98 for the phase found to form continuous layers between the grains of the main phase. At a La/R ratio of about 0.22, the main phase is depleted with La compared with the alloy composition; microscopy also reveals small—undetectable with XRD—amounts of the α-(Fe,Ti) and TiO_2 phases. Both the powder particles and grains of the sintered alloy were rather coarse after milling for 1.5 h, so the latter exhibited a very low H_c of 0.1 kOe. After milling for 10 h, nearly all of the La phase of the starting alloy was oxidized, and the sintering did not lead to any significant densification (Fig. 4). However, the 10 h of milling resulted in uniform particles approximately 1 μm in size, leading to fine, 3–5 μm grains after the sintering (the micrographs are not shown). This refinement may explain the higher H_c of 0.42 kOe. This H_c, however, is still too low—either because the low density leaves too many grain surfaces exposed or because significant amounts of the magnetically soft α-(Fe,Ti) phase and TiO_2 precipitates facilitate reversal of the magnetization. The increased amounts of the α-(Fe,Ti) and TiO_2 phases indicate that the longer milling time led to the oxidation not only of the La phase, but also of a part of the rare-earth elements in the $R(Fe,Ti)_{12}$ phase.

Thus, even though we were apparently able to induce a low-melting-temperature eutectic, and this eutectic allowed for a more complete sintering, the high reactivity of La conflicted with the development of H_c through the refinement of the crystallites in this experiment.

4.2. "Bulk" magnetic hardening

Specific alloy systems such as Sm–Co–Fe–Cu–Zr or Pr–Fe–B–Cu allow for the manufacturing of functional magnets via a simple and less costly alternative to sintering and rapid solidification—via the recrystallization of regularly cast ingots. If formation of the hard magnetic phase is initially suppressed, subsequent heat treatment can be tuned to ensure that the phase crystallizes with the proper morphology. The only known $R(Fe,M)_{12}$ alloy susceptible to bulk hardening is $Sm(Fe,V)_{12}$; it solidifies into a mixture of the α-(Fe, V) and $SmFe_2$ phases and, after controlled crystallization of the $SmFe_{10}V_2$ phase, develops an H_c up to 3.7 kOe [39]. We were able to achieve bulk hardening in alloys prepared from Fe, Ti, and an inexpensive mixture of 65% Ce and 35% La metals (the mixture is close to the naturally occurring ratio of these underused rare-earth elements) utilizing the tendency of La to form low-melting-temperature eutectics, as described in Section 4.1. Fig. 6 shows microstructures of the alloy designed as a hypothetical mixture of the $CeFe_{11}Ti$ and La phases. The as-prepared ingot consisted mostly of bcc α-(Fe,Ti) and RFe_2 phases (the XRD data are not shown). The dhcp La (or La–Ce) phase was also observed, along with a small amount of the $R(Fe,Ti)_{12}$ phase. Differential thermal analysis (DTA) of the as-prepared alloy (Fig. 7, inset) revealed a probable eutectic reaction involving the La–Ce phase at 718 °C (in the binary alloy systems, the eutectic reaction between La and Fe occurs at 780 °C, and that between Ce and $CeFe_2$ occurs at 592 °C).

Heat-treated Ce–La–Fe–Ti alloys develop a microstructure consisting of $CeFe_{11}Ti$ grains surrounded by La-rich phases (Fig. 6(b)). The fine black precipitates were identified as the non-magnetic $TiFe_2$ phase. This microstructure results in obvious magnetic hardening, although because the H_a of the $CeFe_{11}Ti$ phase is only 17 kOe [40] and some of the grains are larger than 10 μm, the H_c is only 0.3 kOe (Fig. 7). A partial replacement of Ce with Sm can increase the H_c to at least 0.5 kOe. Only a small part of the Ce, however, can be replaced; otherwise, crystallization of the $R(Fe,Ti)_{12}$ phase is no longer suppressed in the as-prepared alloys. We also reproduced the bulk hardening in the Sm–Fe–V alloys [39] and attempted to improve the microstructure developing in these alloys by adding La. Although a uniform microstructure of fine, 1–10 μm grains surrounded by a La-rich phase was obtained (Fig. 8, inset), the maximum H_c of 3.3 kOe was not higher than in the earlier report [39]. It may be noted that annealing at different temperatures allowed us to suppress and stabilize the RFe_2

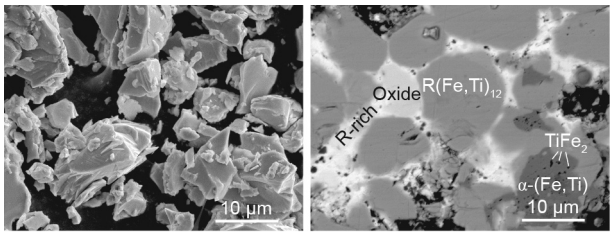

Fig. 5. Micrographs of $(Sm_{0.084}Fe_{0.842}Ti_{0.074})_{95}La_5$ alloy after (a) milling for 1.5 h (secondary electrons image) and (b) subsequent sintering (backscattered electrons image). Black areas in (b) correspond to voids.

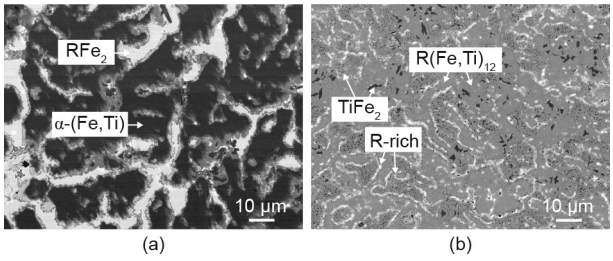

Fig. 6. Backscattered electrons micrographs of $(Ce_{0.09}Fe_{0.83}Ti_{0.08})_{95.5}La_{4.5}$ alloy. (a) As-cast; (b) annealed at 725 °C for 48 h.

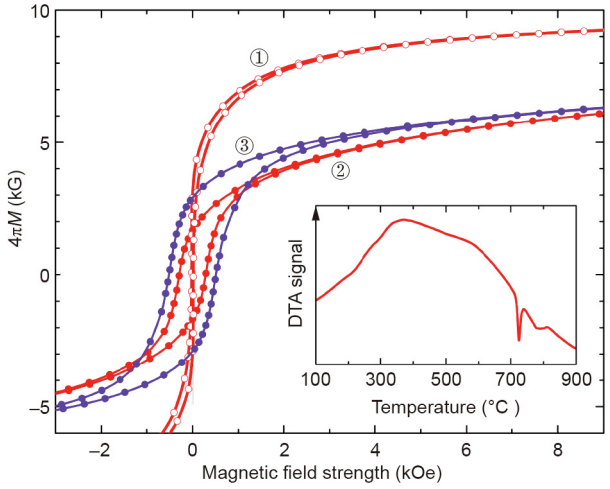

Fig. 7. Room-temperature magnetic hysteresis loops of ① as-cast $(Ce_{0.09}Fe_{0.83}Ti_{0.08})_{95.5}La_{4.5}$ alloy; ② the same alloy annealed at 725 °C for 48 h; ③ $(Ce_{0.07}Sm_{0.02}Fe_{0.83}Ti_{0.08})_{95.5}La_{4.5}$ alloy annealed at 725 °C for 0.5 h. Inset: DTA scan of alloy ①.

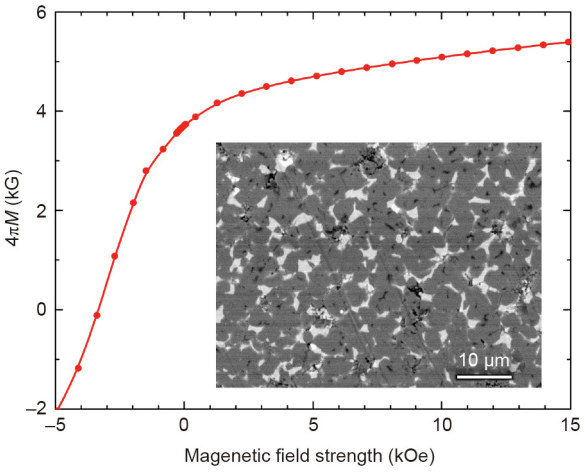

Fig. 8. Room-temperature demagnetization curves of $(Sm_{0.12}Fe_{0.75}V_{0.13})_{98}La_2$ alloy annealed at 700 °C for 20 h. Inset: backscattered electrons micrograph showing $Sm(Fe,V)_{12}$ grains separated by a La-rich phase.

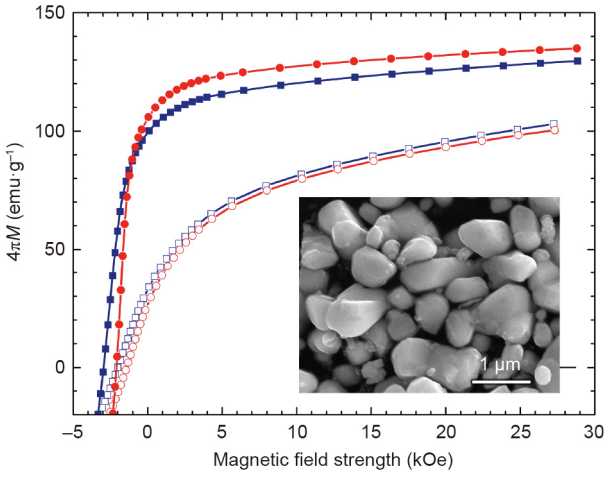

Fig. 9. Room-temperature demagnetization curves of field-oriented $Sm_{0.9}Zr_{0.1}(Fe_{0.75}Co_{0.25})_{11.35}Ti_{0.65}$ particles (nominal composition) measured parallel (filled symbols) and perpendicular (open symbols) to the alignment direction. The particles were prepared via mechanical activation of an oxide-calcium mixture followed by annealing at 1100 °C (blue squares) or 1150 °C (red circles) and washing. Inset: particles synthesized at 1100 °C.

minority phase; the H_c was found to be consistently higher when the RFe_2 phase was present in the alloy.

4.3. Mechanochemistry

Instead of refining the grains or particles of a pre-manufactured alloy, it is possible to obtain ultrafine single crystals directly from elemental components by reducing a mixture of the corresponding oxides with metallic calcium (Ca). Since the calciothermic reduction requires temperatures in excess of 800 °C, special measures must be taken to prevent growth and sintering of the newly synthesized particles. In 1997, 3–8 μm particles of $Nd(Fe,Mo)_{12}$ alloy were obtained by reducing chemically synthesized nanoscale oxide precursors [41]. More recently, a mechanochemical approach, which achieves the initial refinement through mechanical activation, was employed to prepare submicron $(Sm,Ce)(Fe,Co)_{11}Ti$ [42] and $(Sm,Ce,Zr)Fe_{10}Si_2$ [43] particles. The $Sm_{0.7}Zr_{0.3}Fe_{10}Si_2$ particles exhibited a remarkable (for the $ThMn_{12}$-type alloys) combination of susceptibility to magnetic-field alignment and a high H_c of 10.8 kOe; when projected onto a full-density magnet, their $(BH)_{max}$ was 13.8 MG·Oe.

We used mechanochemistry in our attempt to develop an H_c in the "Ti-lean" high-magnetization $Sm_{1-y}Zr_y(Fe,Co)_{12-x}Ti_x$ alloys, which were reviewed in Section 3.5. A blend of Sm_2O_3, ZrO_2, Fe_2O_3, TiO_2, and Co powders was subjected to high-energy ball-milling, together with Ca granules and a CaO powder that was added as a dispersant. The mechanically activated mixture was then annealed for 5 min at 1100–1150 °C to complete the reduction. The alloy particles were collected after washing off the dispersant and byproducts of the synthesis [43]. Fig. 9 presents the magnetization curves recorded for the oriented particles. The H_c of 2–3 kOe was lower than that of the similarly prepared $SmFe_{11}Ti$ particles [42], and the less-than-perfect alignment did not allow for the remanent magnetization that could be expected based on the properties reported for the alloy (Table 1). It is likely that further tuning of the process will more completely realize the high potential of the alloys, although it must be noted that no working procedure has been developed yet to convert the mechanochemically synthesized powders into fully dense permanent magnets.

5. Concluding remarks

This review highlights the wide gap that exists between the excellent intrinsic properties reported for several Fe(Co)-rich $ThMn_{12}$-type compounds and the marginal hard magnetic properties of the corresponding alloys. It may never be possible to synthesize in bulk the RFe_{12} and $R(Fe,Co)_{12}$ compounds that can be stabilized in epitaxially grown thin films. Furthermore, the $x = 0.5$ value for Ti reported in $R_{1-v}Zr_v(Fe,Co)_{12-x}Ti_x$ compounds may be too small to allow the development of functional magnets; a somewhat larger x seems to be needed in order to avoid the presence of a magnetically soft α-Fe phase (the micromagnetics simulations in Ref. [44], which concluded that a few percent of the α-Fe phase can be tolerated, was performed by assuming finer grains than what the real magnets are likely to have). However, even easy-to-synthesize compounds such as $SmFe_{11}Ti$ or $SmFe_{10}Si_2$ seriously underperform in magnetically hard alloys. It is not known yet if they are predisposed to specific lattice defects, and little attention has been paid to this issue so far. It is possible that the infiltration treatment reported in Ref. [29], which is similar to the one that proved to be so effective in improving the Nd-Fe-B magnets, will be the solution.

Acknowledgements

This work was supported by the US Department of Energy, United States (DE-FG02-90ER45413), EU Horizon 2020 Program (686056–NOVAMAG) and Ford Motor Company, United States.

Compliance with ethics guidelines

G.C. Hadjipanayis, A.M. Gabay, A.M. Schönhöbel, A. Martín-Cid, J.M. Barandiaran, and D. Niarchos declare that they have no conflict of interest or financial conflicts to disclose.

References

[1] Hirosawa S. Permanent magnets beyond Nd–Dy–Fe–B. JOM 2015;67(6):1304–5.
[2] Nassar NT, Du X, Graedel TE. Criticality of the rare earth elements. J Industr Ecol 2015;19(6):1044–54.
[3] Buschow KHJ. Permanent magnet materials based on tetragonal rare earth compounds of the type $RFe_{12-x}M_x$. J Magn Magn Mater 1991;100(1–3):79–89.
[4] Bacmann M, Baudelet C, Fruchart D, Gignoux D, Hlil EK, Krill G, et al. Exchange interactions and magneto-crystalline anisotropy in $RFe_{12-x}M_x$ and parent interstitial compounds. J Alloys Compd 2004;383(1–2):166–72.
[5] Wang YZ, Hadjipanayis GC. Magnetic properties of Sm–Fe–Ti–V alloys. J Magn Magn Mater 1990;87(3):375–8.

[6] Schultz L, Schnitzke K, Wecker J. High coercivity in mechanically alloyed Sm–Fe–V magnets with a $ThMn_{12}$ crystal structure. Appl Phys Lett 1990;56(9):868–70.

[7] Yang J, Mao W, Yang Y, Ge S, Zhao Z, Li F. Nitrogenation of the magnetic compound $R(Fe, M)_{12}$. J Appl Phys 1998;83(4):1983–7.

[8] Wang Y, Hadjipanayis GC, Kim A, Liu NC, Sellmyer DJ. Magnetic and structural studies in Sm–Fe–Ti magnets. J Appl Phys 1990;67(9):4954–6.

[9] Ke L, Johnson DD. Intrinsic magnetic properties in $R(Fe_{1-x}, Co_x)_{11}TiZ$ (R = Y and Ce; Z = H, C, and N). Phys Rev B 2016;94(2):024423.

[10] Körner W, Krugel G, Elsässer C. Theoretical screening of intermetallic $ThMn_{12}$-type phases for new hard-magnetic compounds with low rare earth content. Sci Rep 2016;6(1):24686.

[11] Fukazawa T, Akai H, Harashima Y, Miyake T. First-principles study of intersite magnetic couplings in $NdFe_{12}$ and $NdFe_{12}X$ (X = B, C, N, O, F). J Appl Phys 2017;122(5):053901.

[12] Delange P, Biermann S, Miyake T, Pourovskii L. Crystal-field splittings in rare-earth-based hard magnets: an *ab initio* approach. Phys Rev B 2017;96(15):155132.

[13] Harashima Y, Fukazawa T, Kino H, Miyake T. Effect of R-site substitution and pressure on stability of RFe_{12}: a first-principles study. J Appl Phys 2018;124(16):163902.

[14] Harashima Y, Terakura K, Kino H, Ishibashi S, Miyake T. First-principles study on stability and magnetism of $NdFe_{11}M$ and $NdFe_{11}MN$ for M = Ti, V, Cr, Mn, Fe Co, Ni, Cu, Zn. J Appl Phys 2016;120(20):203904.

[15] Skelland C, Ostler T, Westmoreland SC, Evans RFL, Chantrell RW, Yano M, et al. Probability distribution of substituted titanium in RT_{12} (R = Nd and Sm; T = Fe and Co) structures. IEEE Trans Magn 2018;54(11):1–5.

[16] Cadieu FJ, Hegde H, Navarathna A, Rani R, Chen K. High-energy product $ThMn_{12}$ Sm–Fe–T and Sm-Fe permanent magnets synthesized as oriented sputtered films. Appl Phys Lett 1991;59(7):875–7.

[17] Hirayama Y, Takahashi YK, Hirosawa S, Hono K. $NdFe_{12}N_x$ hard-magnetic compound with high magnetization and anisotropy field. Scr Mater 2015;95:70–2.

[18] Sato T, Ohsuna T, Yano M, Kato A, Kaneko Y. Permanent magnetic properties of $NdFe_{12}N_x$ sputtered films epitaxially grown on V buffer layer. J Appl Phys 2017;122(5):053903.

[19] Hirayama Y, Takahashi YK, Hirosawa S, Hono K. Intrinsic hard magnetic properties of $Sm(Fe_{1-x}Co_x)_{12}$ compound with the $ThMn_{12}$ structure. Scr Mater 2017;138:62–5.

[20] Grössinger R, Krewenka R, Sun XK, Eibler R, Kirchmayr HR, Buschow KHJ. Magnetic phase transitions and magnetic anisotropy in $Nd_2Fe_{14-x}Co_xB$ compounds. J Less Common Met 1986;124(1–2):165–72.

[21] Hirosawa S, Matsuura Y, Yamamoto H, Fujimura S, Sagawa M, Yamauchi H. Magnetization and magnetic anisotropy of $R_2Fe_{14}B$ measured on single crystals. J Appl Phys 1986;59(3):873–9.

[22] Fukuda Y, Fujita A, Shimotomai M. Magnetic properties of monocrystalline $Nd_2(Fe,Co,Ni)_{14}B$. J Alloys Compd 1993;193(1–2):256–8.

[23] Suzuki S, Kuno T, Urushibata K, Kobayashi K, Sakuma N, Washio K, et al. A $(Nd, Zr)(Fe,Co)_{11.5}Ti_{0.5}N_x$ compound as a permanent magnet material. AIP Adv 2014;4(11):117131.

[24] Suzuki S, Kuno T, Urushibata K, Kobayashi K, Sakuma N, Washio K, et al. A new magnet material with $ThMn_{12}$ structure: $(Nd_{1-x}Zr_x)(Fe_{1-y}Co_y)_{11+z}Ti_{1-z}N_\alpha$ (α = 0.6–1.3). J Magn Magn Mater 2016;401:259–68.

[25] Gabay AM, Hadjipanayis GC. Recent developments in RFe_{12}-type compounds for permanent magnets. Scr Mater 2018;154:284–8.

[26] Hagiwara M, Sanada N, Sakurada S. Effect of Y substitution on the structural and magnetic properties of $Sm(Fe_{0.8}Co_{0.2})_{11.4}Ti_{0.6}$. J Magn Magn Mater 2018;465:554–8.

[27] Tozman P, Sepehri-Amin H, Takahashi YK. Hirosawa S, Hono K. Intrinsic magnetic properties of $Sm(Fe_{1-x}Co_x)_{11}Ti$ and Zr-substituted $Sm_{1-y}Zr_y(Fe_{0.8}Co_{0.2})_{11.5}Ti_{0.5}$ compounds with $ThMn_{12}$ structure toward the development of permanent magnets. Acta Mater 2018;153:354–63.

[28] Kuno T, Suzuki S, Urushibata K, Kobayashi K, Sakuma N, Yano M, et al. $(Sm,Zr)(Fe,Co)_{11.0-11.5}Ti_{1.0-1.5}$ compounds as new permanent magnet materials. AIP Adv 2016;6(2):025221.

[29] Ogawa D, Xu XD, Takahashi YK, Ohkubo T, Hirosawa S, Hono K. Emergence of coercivity in $Sm(Fe_{0.8}Co_{0.2})_{12}$ thin films via eutectic alloy grain boundary infiltration. Scr Mater 2019;164:140–4.

[30] Nakagawa R, Doi M, Shima T. Effect of nonmagnetic cap layers for Nd–Fe–B thin films with small addition of rare-earth element. IEEE Trans Magn 2015;51(11):2104904.

[31] Wang YZ, Hadjipanayis GC. Effect of nitrogen on the structural and magnetic properties of intermetallic compounds with the $ThMn_{12}$ structure. J Appl Phys 1991;70(10):6009–11.

[32] Yang J, Dong S, Yang Y, Cheng B. Structural and magnetic properties of $RFe_{10.5}V_{1.5}N_x$. J Appl Phys 1994;75(6):3013–6.

[33] Fu JB, Yu X, Qi ZQ, Yang WY, Liu SQ, Wang CS, et al. Magnetic properties of Nd $(Fe_{1-x}Co_x)_{10.5}M_{1.5}$ (M = Mo and V) and their nitrides. AIP Adv 2017;7(5):056202.

[34] Zhou C, Pinkerton FE, Herbst JF, inventors; GM Global Technology Operations LLC, assignee. Cerium-iron-based magnetic compounds. United States patent US201313786807. 2017 Jan 17.

[35] Kobayashi K, Suzuki S, Kuno T, Urushibata K, Sakuma N, Yano M, et al. The stability of newly developed $(R,Zr)(Fe,Co)_{12-x}Ti_x$ alloys for permanent magnets. J Alloys Compd 2017;694:914–20.

[36] Gabay AM, Hadjipanayis GC. $ThMn_{12}$-type structure and uniaxial magnetic anisotropy in $ZrFe_{10}Si_2$ and $Zr_{1-x}Ce_xFe_{10}Si_2$ alloys. J Alloys Compd 2016;657:133–7.

[37] Gjoka M, Psycharis V, Devlin E, Niarchos D, Hadjipanayis G. Effect of Zr substitution on the structural and magnetic properties of the series $Nd_{1-x}Zr_xFe_{10}Si_2$ with the $ThMn_{12}$ type structure. J Alloys Compd 2016;687:240–5.

[38] Gabay AM, Cabassi R, Fabbrici S, Albertini F, Hadjipanayis GC. Structure and permanent magnet properties of $Zr_{1-x}R_xFe_{10}Si_2$ alloys with R = Y, La, Ce, Pr and Sm. J Alloys Compd 2016;683:271–5.

[39] Sugimoto S, Shimono T, Nakamura H, Kagotani T, Okada M, Homma M. Magnetic properties and microstructures of the $(SmFe_{10}V_2)_{1-x}$–$(Sm_2Fe_{17})_x$ cast alloys. Mater Chem Phys 1995;42(4):298–301.

[40] Zhou C, Pinkerton FE, Herbst JF. Magnetic properties of $CeFe_{11-x}Co_xTi$ with $ThMn_{12}$ structure. J Appl Phys 2014;115(17):17C716.

[41] Su MZ, Liu SF, Qian XL, Lin JH. An alternative approach to the finely crystalline powder of rare earth-transition metal alloys. J Alloys Compd 1997;249(1–2):229–33.

[42] Gabay AM, Martín-Cid A, Barandiaran JM, Salazar D, Hadjipanayis GC. Low-cost $Ce_{1-x}Sm_x(Fe,Co,Ti)_{12}$ alloys for permanent magnets. AIP Adv 2016;6(5):056015.

[43] Gabay AM, Hadjipanayis GC. Mechanochemical synthesis of magnetically hard anisotropic $RFe_{10}Si_2$ powders with R representing combinations of Sm, Ce and Zr. J Magn Magn Mater 2017;422:43–8.

[44] Fischbacher J, Kovacs A, Gusenbauer M, Oezelt H, Exl L, Bance S, et al. Micromagnetics of rare-earth efficient permanent magnets. J Phys D Appl Phys 2018;51(19):193002.